



OPEN

DATA DESCRIPTOR

Multi-wavelength global maps of Jupiter and Saturn using Cassini imaging system data

Xinyue Wang¹✉, Liming Li², Xun Jiang¹ & Robert A. West³

The Imaging Science Subsystem onboard the Cassini spacecraft recorded numerous high-quality images of Jupiter and Saturn at various wavelengths, from ultraviolet to near-infrared, during its 20-year mission from 1997 to 2017. Using these images, we have developed global maps of Jupiter and Saturn across multiple wavelengths. These maps reveal the global atmospheric structures of Jupiter and Saturn, offering a comprehensive tool to study the physical and dynamic processes of these atmospheric systems on a global scale. Additionally, these multi-wavelength maps, which probe different pressure systems within the atmospheres, help to explore the vertical structure of these processes. Moreover, global maps at different times enable tracking the movement of dynamic phenomena (e.g., clouds, storms, vortices, eddies, waves, and turbulence), thereby enhancing our understanding of atmospheric dynamics on the giant planets.

Background & Summary

Global maps are essential for scientific studies of astronomical bodies. Consequently, creating global maps of planets and satellites is one of primary objectives of planetary missions. Significant progress has been made in developing and archiving global geological maps for terrestrial bodies in our solar system, with support from programs and systems such as the Planetary Geologic Mapping Program by the United States Geological Survey, the Geosciences Node of the Planetary Data System, and the Geographic Information Systems of the Ronald Greeley Center for Planetary Studies. However, for giant planets, their solid surfaces, if they exist, are obscured by thick atmospheres, making it infeasible to create geological maps. Instead, global atmospheric maps can be constructed, despite challenges posed by temporally varying cloud morphology. Currently, publicly available global maps of giant planets are limited, except for a few maps of Jupiter. The scarcity of well-organized global maps of giant planets is primarily due to the limited number of missions and observations capable of global imaging.

The long-term, multi-wavelength observations from the Cassini mission¹ provide an exceptional opportunity to develop global maps of Jupiter and Saturn. Cassini was an international mission supported by NASA, the European Space Agency (ESA), and the Italian Space Agency (ASI). Launched in 1997, the spacecraft completed its mission in 2017. Cassini's primary objective was to observe the Saturn system, including Saturn's atmosphere, rings, and satellites. Before its insertion into Saturn's orbit in 2004, Cassini conducted a strategic flyby of Jupiter in 2000–2001.

The Cassini spacecraft carried 12 scientific instruments with distinct objectives. In this study, we utilize data from the Imaging Science Subsystem (ISS)². The Cassini ISS is a two-dimensional imaging system consisting of two framing cameras: a narrow-angle reflecting telescope with a square field of view (FOV) of 0.35° across, and a wide-angle refractor with a FOV of 3.5° across. The narrow-angle camera (NAC) captures high-spatial-resolution images, while the wide-angle camera (WAC) provides images with broader spatial coverage. Both NAC and WAC images are used to generate maps at different spatial resolutions, which depend on the camera and the distance between the spacecraft and its target.

The Cassini ISS cameras are equipped with multiple filters covering a range from ultraviolet to near-infrared. The optical properties of these filters are detailed in the ISS introductory paper². Filters corresponding to weak, medium, and strong methane absorption bands (MT1/2/3) are crucial for distinguishing vertical atmospheric

¹Department of Earth and Atmospheric Sciences, University of Houston, Houston, TX, 77004, USA. ²Department of Physics, University of Houston, Houston, TX, 77004, USA. ³Jet Propulsion Laboratory, California Institute of Technology, Pasadena, CA, 91109, USA. ✉e-mail: xwang216@cougarnet.uh.edu

Planet	Filter (Wavelength)	Number of Maps	Observational Time	Spatial Resolution
Jupiter	BL1 (455 nm)	6	Dec. 7–16, 2000	103–145 km/pixel
Jupiter	CB2 (750 nm)	6	Dec. 7–16, 2000	103–145 km/pixel
Jupiter	MT3 (889 nm)	4	Dec. 7–16, 2000	103–145 km/pixel
Jupiter	UV1 (264 nm)	3	Dec. 7–14, 2000	227–289 km/pixel
Saturn	MT2 (728 nm)	1	Oct. 23, 2009	110–111 km/pixel
Saturn	RED (647 nm)	1	Aug. 12, 2011	161 km/pixel
Saturn	GRN (568 nm)	1	Aug. 12, 2011	161 km/pixel
Saturn	BL1 (463 nm)	1	Aug. 12, 2011	161 km/pixel
Saturn	RGB	2	Aug. 12, 2011	161 km/pixel

Table 1. Basic Information of the global maps of Jupiter and Saturn. *Note:* The wavelength corresponding to each filter represents the effective wavelength. The BL1 filter wavelength for Jupiter corresponds to the narrow-angle camera, while the BL1 filter wavelength for Saturn corresponds to the wide-angle camera in the ISS. Each global map of Jupiter and Saturn is constructed using several ISS images taken over 8–11 hours, with varying spatial resolutions. “RGB” refers to color global maps composed of three individual global maps captured using the RED, GRN, and BL1 filters, respectively. The two RGB maps of Saturn represent the original map and the feature-contrast-enhanced map, respectively. More information on these global maps of Jupiter and Saturn is available on the Planetary Atmospheres Node of NASA’s Planetary Data System (PDS) website (https://atmos.nmsu.edu/data_and_services/atmospheres_data/Cassini/sat_global_map.html).

features. The three continuum filters (CB1/2/3), associated with the methane filters, mainly probe the upper visible clouds (primarily NH_3) on Jupiter and Saturn. Additionally, three ultraviolet filters (UV1/2/3) are sensitive to relatively high-altitude clouds and hazes on these planets. Images recorded using blue (BL1), green (GRN), and red (RED) filters can be combined to create color global maps of Jupiter and Saturn. However, sometimes the images taken with the three color filters are insufficient to create complete color maps. Utilizing the available ISS images archived in the Planetary Data System, we have generated several global maps at different wavelengths for Jupiter and Saturn, as summarized in Table 1.

These global maps will significantly enhance the exploration of the atmospheric systems of Jupiter and Saturn, with a focus on the global survey and spatio-temporal variability of these systems. First, the global maps of Jupiter and Saturn will enable us to survey key dynamical processes, such as clouds, storms, vortices, eddies, waves, and turbulence, on these two gas giant planets. Second, the global maps based on images recorded with different filters can help us understand the vertical structure of these atmospheric processes. For example, the CB2 images primarily capture the top visible clouds (NH_3) at pressure levels around 750 mbar on Jupiter³. Additionally, the ISS images recorded at the MT3 and UV1 filters probe pressure levels above those sensed by the CB2 images. The UV1 images mainly detect stratospheric hazes around 50 mbar^{3,4}, which is near Jupiter’s tropopause at ~100 mbar. These stratospheric hazes do not significantly affect opacity at the wavelength of the MT3 filter⁵, so methane gas absorption plays a critical role in determining the optical depth at the MT3 wavelength. Investigations into the optical depth of Jupiter’s atmosphere at the MT3 wavelength⁶ suggest that MT3 images probe pressure levels around 300 mbar. Therefore, examining atmospheric processes using these global maps at different filters can provide valuable insights into their vertical structure. Finally, Jupiter’s global maps at different times (see Table 1) offer an opportunity to study the temporal variations in Jupiter’s atmosphere over relatively short timescales.

Methods

In this section, we discuss the methodology for creating high-spatial-resolution global maps of Jupiter and Saturn using images captured by multiple filters of the ISS onboard the Cassini spacecraft. The raw ISS images are publicly available on the NASA Planetary Data System (PDS) (<https://pds-imaging.jpl.nasa.gov/volumes/iss.html>).

To resolve fine structures in the atmospheres of Jupiter and Saturn, we use high-spatial-resolution images for creating the global maps. For Jupiter, we only use ISS images with spatial resolutions better than 150 km/pixel, except for those recorded with ultraviolet (UV) filters. One degree at Jupiter’s equator corresponds to approximately 1250 km. Thus, the global maps, based on selected images with spatial resolutions better than 150 km/pixel, have a spatial resolution of approximately 0.1 degrees in both latitude and longitude. The UV images were recorded at 512×512 pixels, while images from other filters were recorded at 1024×1024 pixels. As a result, the spatial resolution of the UV images is lower than that of images recorded with other filters. Therefore, we relaxed the criterion for selecting UV images to 300 km/pixel for creating global maps. Based on the above criteria, we searched the complete Cassini dataset and found suitable images to create six global maps with the BL1 filter, six global maps with the CB2 filter, four global maps with the MT3 filter, and three global maps with the UV1 filter (see Table 1).

Creating global maps of Saturn is challenging due to its rings. First, the rings cast shadows on Saturn. Specifically, when the time is far from the equinox, the rings’ shadow can cover more than half of Saturn’s surface area. Second, the rings can obstruct the spacecraft’s (Cassini) view, preventing some areas of Saturn from being recorded by the Cassini/ISS. Third, sunlight scattering from the rings introduces difficulties in removing solar illumination from Saturn’s images.

To address the first two challenges (shadowing and obstruction by the rings), we select the best datasets to maximize the observed sunlight-illuminated area. One option is to use images recorded around the Northern Spring Equinox (August 2009), during which the rings’ shadow forms a line at the equator, providing the largest

sunlight-illuminated area of Saturn's atmosphere in the ISS images. Additionally, we need to consider the spacecraft's viewing geometry. The Cassini spacecraft should be positioned around the equatorial plane (i.e., rings plane) to minimize obstruction by the rings. Moreover, the phase angle (i.e., the Sun-Saturn-Cassini angle) should not be too large to ensure that the sunlight-illuminated areas are sufficient for creating global maps. Lastly, we focus on images with high spatial resolution to capture fine structures in Saturn's atmosphere. For Saturn, images with spatial resolutions better than 200 km/pixel are suitable for effectively capturing atmospheric features.

We searched the ISS dataset and found one group of images recorded with the second continuum filter (CB2) and the medium methane-absorption filter (MT2) that satisfy the aforementioned conditions. However, some images from the CB2 filter cannot be navigated accurately. Therefore, we only processed the MT2 images to create the global map. It is important to emphasize that this is a global map of Saturn with the best global coverage. Unfortunately, Cassini ISS did not record enough images around the Spring Equinox using the three color filters (i.e., RED, GRN, and BL1). Consequently, we are unable to generate color maps of Saturn, which are typically composed of red, green, and blue images, using images recorded around the Spring Equinox.

We then conducted a search for additional images taken at times other than the Spring Equinox in 2009 to create color maps. Eventually, we identified a group of red, green, and blue images recorded by the ISS in 2011, which can be utilized to generate a high-spatial-resolution global color map, despite some areas near the equator being obscured by the rings. Given that the Cassini spacecraft recorded a significantly larger number of high-spatial-resolution images of Saturn compared to other spacecraft, the global color map of Saturn not only has excellent spatial resolution but also extensive spatial coverage. To enhance the contrast of the global color map, we adjusted the ranges of the red, green, and blue global maps and also created a contrast-enhanced global color map. The basic steps involved in creating the global maps of Jupiter and Saturn are outlined below.

First, we conducted a search and selection process to identify suitable ISS images. We downloaded the LOG and Label files of the ISS images from the PDS. Subsequently, we utilized our own codes to search and select these high-spatial-resolution images for the purpose of generating global maps. Additionally, the PDS offers an online image-searching tool (accessible at opus.pds-rings.seti.org). This PDS search tool can also be employed to search for ISS images suitable for creating global maps. Upon identifying the images for creating global maps, we downloaded the raw ISS images from the PDS website. Subsequently, we employed navigation software developed by the ISS team to perform navigation. The navigated backplanes, which provide latitude and longitude positions for the pixels on the ISS raw images, can be also generated using the ISS software and validated using the USGS Integrated Software for Imagers and Spectrometers (ISIS) (accessible at <https://isis.astrogeology.usgs.gov/7.0.0/index.html>). Since the navigation software developed by the Cassini ISS team is not actively maintained following the conclusion of the Cassini mission, we recommend using the USGS ISIS for navigation purposes. Based on the navigated planes of longitude and latitude, we can project the ISS images onto map pieces with coordinates of longitude and latitude. For map projection, we use cylindrical projection because we are creating global maps from pole to pole. There are standard IDL/MATLAB routines that triangulate the pixel points in the raw image as projected on the new latitude/longitude coordinate system (e.g., see <https://www.mathworks.com/help/map/summary-and-guide-to-projections.html>). Finally, the map pieces covering different latitudes and longitudes are combined to create the global maps. Generally, artificial seams appear around the boundaries of map pieces when combining them to form global maps. These artificial seams are mainly caused by solar illumination. The classical Minnaert correction⁷ works well for removing the solar illumination and the related artificial seams in Jupiter's global maps. However, for Saturn, the combination of solar illumination and the scattering from its rings makes the artificial seams more complicated. An empirical approach, developed in previous studies^{8–10}, is used to remove these artificial seams.

Data Records

The global map data products of Jupiter and Saturn are available in both PNG and FITS formats, facilitating easy browsing and further processing, respectively. Additionally, the basic details of the global maps and the corresponding ISS raw images are summarized in tables. All data products are archived on the Planetary Atmospheres Node of the NASA PDS (https://atmos.nmsu.edu/data_and_services/atmospheres_data/Cassini/sat_global_map.html)¹¹.

In this context, we primarily focus on introducing the global map products of Jupiter and Saturn (see Table 1 for a summary of the global maps). The spatial resolutions of the ISS images at BL1, CB2, and MT3 are better than 150 km/pixel. It is worth noting that one degree at Jupiter's equator is approximately equivalent to 1250 km. Therefore, the created global maps have a spatial resolution of 0.1° in both latitude and longitude. Figure 1 provides an example of these high-spatial-resolution global maps. It should be noted that seams are present when combining different map pieces into a global map, and these should be taken into account when analyzing the global maps. Panel B of Fig. 1 highlights an example of such seams, which correspond to the boundaries of map pieces. Discontinuities in features can be observed across these boundaries. While the effects of solar illumination have been removed to reduce these discontinuities, they could not be entirely eliminated. This is primarily because small-scale clouds evolve on a timescale comparable to the separation between map pieces (~1 hour), causing the same clouds to appear differently in different map pieces.

The ISS images captured with ultraviolet (UV) filters generally have lower spatial resolutions compared to those taken with other ISS filters, as previously discussed. Figure 2 illustrates a global map derived from the UV1 images. To our knowledge, publicly available global maps of Jupiter at ultraviolet wavelengths have not been found. Therefore, the UV global maps produced in this project are likely the first of their kind at ultraviolet wavelengths.

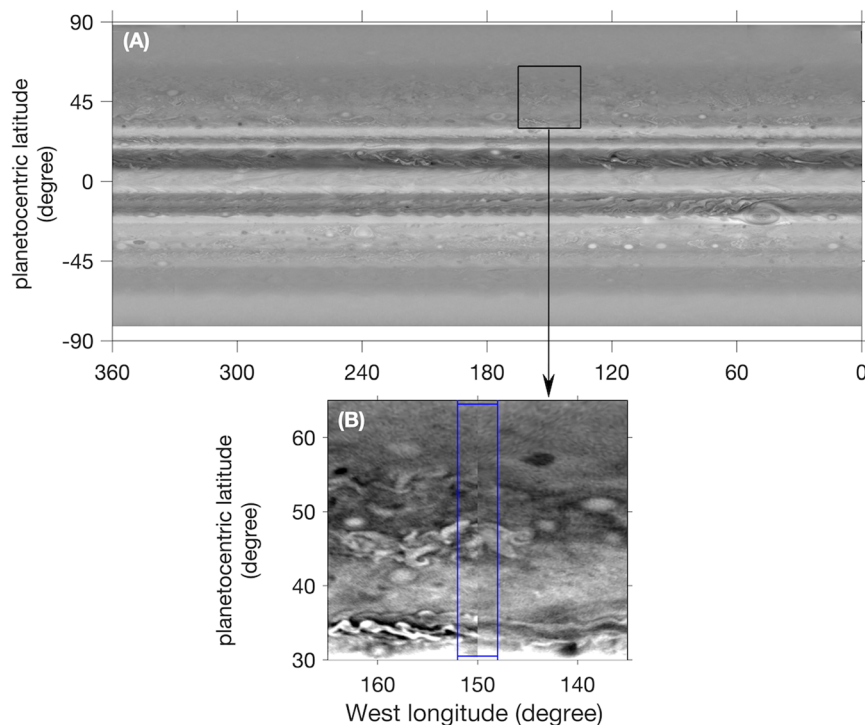


Fig. 1 A global map of Jupiter created using ISS images taken at the BL1 filter (~ 455 nm). **(A)** A global map. The global map consists of a map of the Northern Hemisphere and a map of the Southern Hemisphere. Each hemispheric map is based on eight images captured by the ISS on December 14, 2000, with a spatial resolution of ~ 120 km/pixel and a time interval of \sim one hour. Each ISS image covers approximately 40–50 degrees in longitude, and the combination of these eight images provides complete longitudinal coverage. The blank areas in the polar region represent observational gaps. **(B)** A map section. This map section, outlined by the black box in panel A, highlights a vertical seam generated during the process of combining different map pieces into a global map. The seam, located at longitude 150°, is emphasized within a blue box.

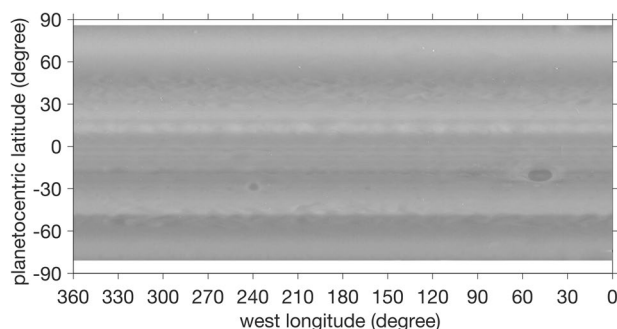


Fig. 2 A global map of Jupiter created using ISS images taken at the UV1 filter (~ 264 nm). The global map consists of a map of the Northern Hemisphere and a map of the Southern Hemisphere. Each hemispheric map is based on seven images captured by the ISS on December 6, 2000, with a spatial resolution of ~ 285 km/pixel and a time interval of ~ 1 hour and 40 minutes. Each ISS image covers ~ 50 – 60 degrees in longitude, and the combination of these seven images provides complete longitudinal coverage. The blank areas in the polar region represent observational gaps.

Jupiter's global maps at different wavelengths correspond to various pressure levels within the atmosphere. Therefore, the global maps generated at different filters/wavelengths are valuable tools for scientists investigating the vertical structure of Jupiter's atmosphere. Figure 3 compares Jupiter's global maps captured using the BL1, CB2, MT3, and UV1 filters, illustrating the distinct appearances of Jupiter's atmosphere across different wavelengths.

We also generated multiple global maps of Jupiter for each of the four ISS filters (BL1, CB2, MT3, and UV1). This collection of global maps, captured at different times, is a valuable resource for scientists studying the temporal variations of atmospheric phenomena. Figure 4 displays six global maps obtained using the CB2 filter. These six maps, spanning from December 6 to December 14, 2000, provide an opportunity to study temporal

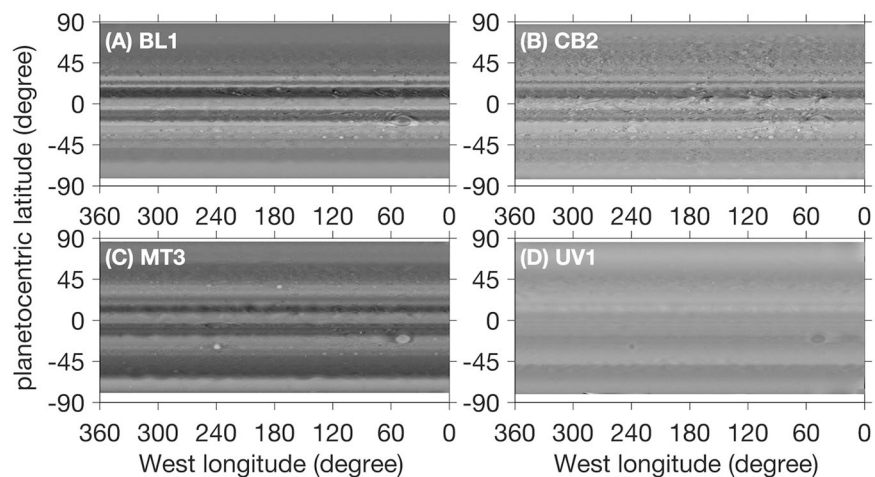


Fig. 3 Global maps of Jupiter created using ISS images recorded at four different filters. Each global map consists of a map of the Northern Hemisphere and a map of the Southern Hemisphere. All the images used to generate these global maps were recorded by the Cassini ISS on December 7, 2000. The time intervals between the four global maps are approximately 1–3 minutes, making them quasi-simultaneous.

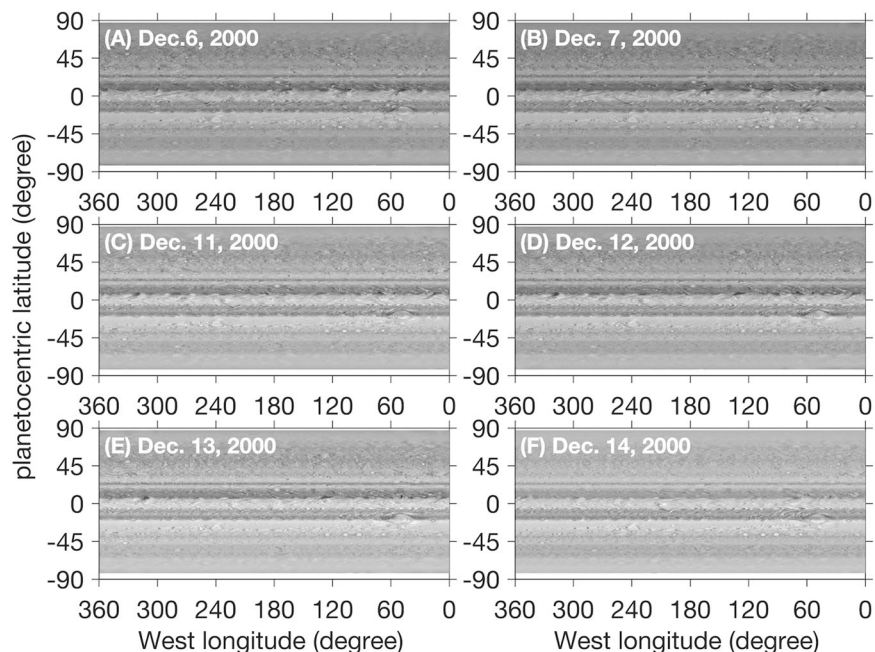


Fig. 4 Jupiter's global maps at different times. These global maps are created using ISS images taken with the CB2 filter (~750 nm). Each global map consists of a map of the Northern Hemisphere and a map of the Southern Hemisphere.

changes in Jupiter's atmosphere on relatively short time scales, such as daily variability. Additionally, these images can be used to track the movements of atmospheric processes. In particular, tracking cloud features is commonly used to measure Jupiter's zonal winds.

Figure 5 highlights an intriguing region on Jupiter, extracted from the global maps shown in Fig. 4. Within this region, three vortices of distinct types are identified in panel A of Fig. 5: a dark vortex in the top left, a ringed vortex in the center, and a white vortex in the bottom right. The six panels, spanning the period from December 6 to December 14, 2000, chronicle the dynamic interactions among these vortices. Notably, the dark vortex in the top left was destroyed during the interaction. This sequence provides valuable insights into the vortex dynamics within Jupiter's atmosphere.

Generating global maps of Saturn is challenging due to the presence of its rings, which can cause issues such as obscured views and solar shadowing (see the “Method” section for details). Consequently, there are very few published global maps of Saturn. Despite the availability of thousands of images captured by the Cassini ISS during its extended mission from 2004 to 2017, selecting suitable images for creating global maps remains a difficult

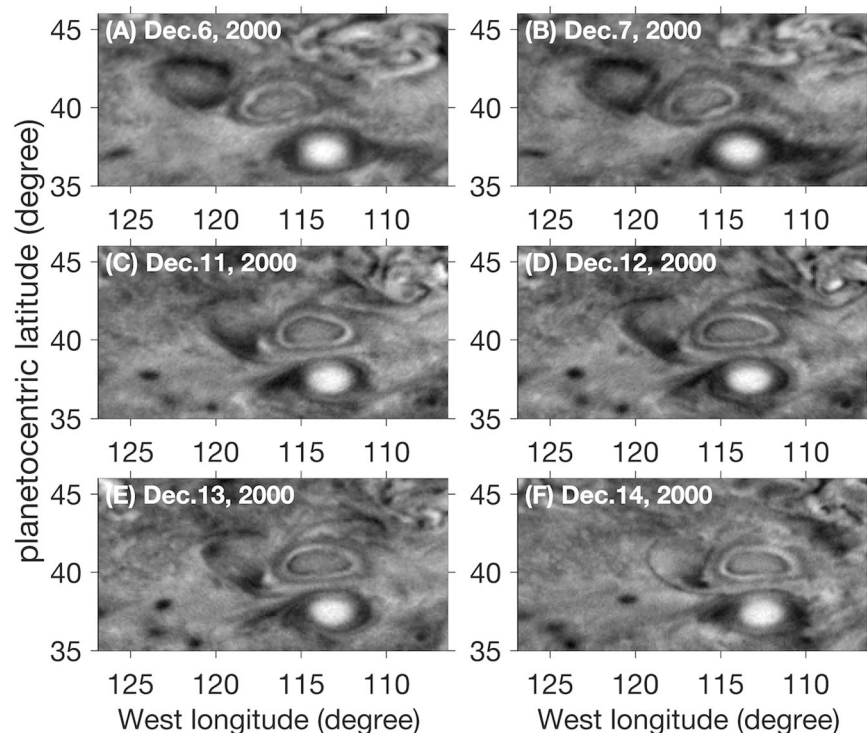


Fig. 5 An interesting region showing vortex dynamics. This region spans latitudes from 35°N to 46°N and longitudes from 106.5° to 127°. The six panels come from the six global maps presented in Fig. 4, respectively.

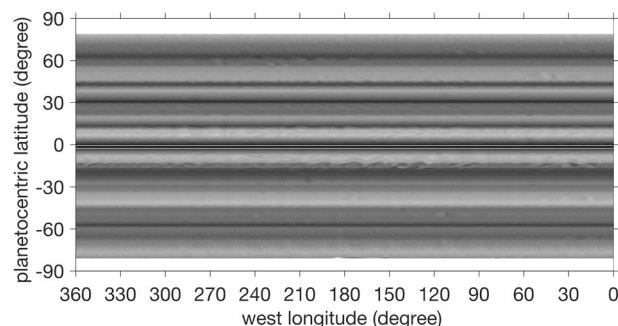


Fig. 6 Saturn's global map displaying the best spatial coverage. The raw ISS images used to create this global map were captured by the ISS MT2 filter (~727 nm) on October 23, 2009. These raw images have a spatial resolution of ~149 km/pixel. The global map is composed of 11 raw images. Typically, we require 5–8 images with good spatial coverage to construct a global map. In this case, we have selected images taken around the equinox to achieve optimal global coverage. However, the ISS recorded these images around the NH Spring Equinox at a high phase angle of ~110 degrees. This high phase angle results in relatively small sun-illuminated areas per image, spanning ~30–40 degrees in longitude. Therefore, we must combine 11 images to cover the entire longitude range from 0 to 360 degrees.

task. After a thorough examination of the ISS dataset, we identified a specific set of images captured by Cassini/ISS using the medium methane-absorption filter (MT2) that was suitable for creating global maps. By processing these MT2 images, we produced the global map shown in Fig. 6.

The MT2 images were recorded in October 2009, near the Northern Hemisphere's Spring Equinox (August 2009). During this period, the sub-solar latitude was very close to the equator, at approximately 1.1°N. Consequently, the shadow cast by the rings appeared as a narrow band near the equator (shown by the thin white line below the equator in Fig. 6). Additionally, the viewing geometry of the Cassini spacecraft was exceptionally favorable for observing Saturn's atmosphere, with a sub-Cassini latitude of approximately 0.4°N. As a result, the rings only obstructed a narrow band of latitude (indicated by the thin gray line around the equator in Fig. 6). The global maps shown in Fig. 6 likely represent the first high-spatial-resolution global maps with optimal spatial coverage of Saturn's atmosphere.

Unfortunately, the Cassini ISS did not capture enough images using the three color filters (RED, GRN, and BL1) around the Northern Hemisphere's Spring Equinox. As a result, it was not possible to generate color maps

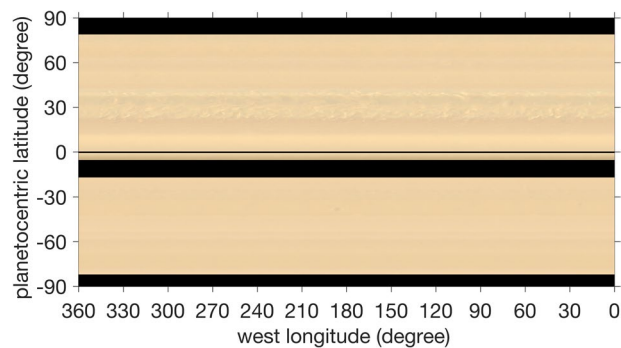


Fig. 7 Saturn's global color map created using global maps at red, green, and blue wavelengths. The global maps at the red, green, and blue channels are based on ISS images recorded with the RED (647 nm), GRN (568 nm), and BL1 (463 nm) filters, respectively. Each global map consists of 5 ISS images captured on August 11, 2011, with a spatial resolution of ~ 161 km/pixel and a time separation of ~ 2.1 hours. Due to the unavailability of RGB images near the Northern Spring Equinox for maximizing global coverage, we selected these RGB images as they can make the global color map with the best spatial coverage among all Cassini RGB images. The selected images were taken at a sub-solar latitude of 10.7°N and a sub-Cassini latitude of 0.2°N . The relatively large sub-solar latitude (10.7°N) results in the shadow cast by the rings covering a latitude band of $\sim 5\text{--}15^\circ\text{S}$ (visible as the wide black area near the equator in the Southern Hemisphere). Conversely, the small sub-Cassini latitude (0.2°N) makes that the rings only obstruct a very narrow latitude band around the equator (illustrated by the thin black line). The black regions in the polar regions indicate observational gaps.

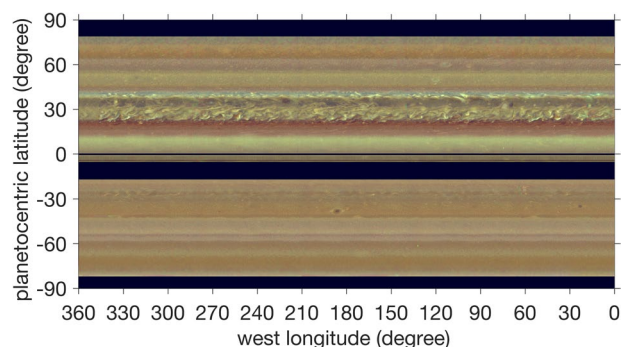


Fig. 8 Same as Fig. 7 except for enhancing the contrast of the global color map.

of Saturn with optimal spatial coverage, as shown in Fig. 6. However, by expanding our search to include images taken at other times, we discovered a set of red, green, and blue images recorded by the ISS in 2011. Although some areas near the equator were obscured by the rings and their shadow, these images allowed us to create a high-spatial-resolution global color map of Saturn, as depicted in Fig. 7. A giant convective storm erupted at approximately 32°N in Saturn's Northern Hemisphere in December 2010^{12–14}. The bright clouds generated by the storm spread longitudinally with the background zonal winds, encircling the entire planet to form a distinct latitudinal band. In the meridional direction, these bright clouds expanded much farther southward than northward^{15–18}, resulting in the latitudinal band of bright clouds having northern and southern boundaries at approximately 40°N and 20°N , respectively. This latitudinal band of bright clouds is depicted in the global map shown in Fig. 7, which is based on images recorded by the Cassini ISS in August 2011.

Given that the Cassini spacecraft captured a significantly larger number of high-spatial-resolution images than other missions, the global color map presented in Fig. 7 is likely the first of its kind. To enhance the contrast of the global color map, we adjusted the ranges of the red, green, and blue global maps and created a contrast-enhanced version, shown in Fig. 8. This contrast-enhanced color map improves the visibility of relatively small atmospheric phenomena compared to the original map.

Technical Validation

The uncertainty in creating global maps of Jupiter and Saturn primarily stems from the process of navigating the ISS raw images. In this study, we used mature navigation software developed by the ISS team, which has been validated by the USGS ISIS. The basic concept behind navigating these hemispheric and global ISS images, which are used to create the global maps, is to align the observed planetary limb (in the image plane) with its predicted location. Since the hemispheric and global images have clearly visible limbs, the navigation procedure generally achieves a precision of less than one pixel, which corresponds to about 0.1° in longitude and latitude at the equator for Jupiter's global maps, except for UV images ($\sim 0.2^\circ$ at the equator). For Saturn, the uncertainty is about $0.1\text{--}0.15^\circ$ in longitude and latitude at the equator.

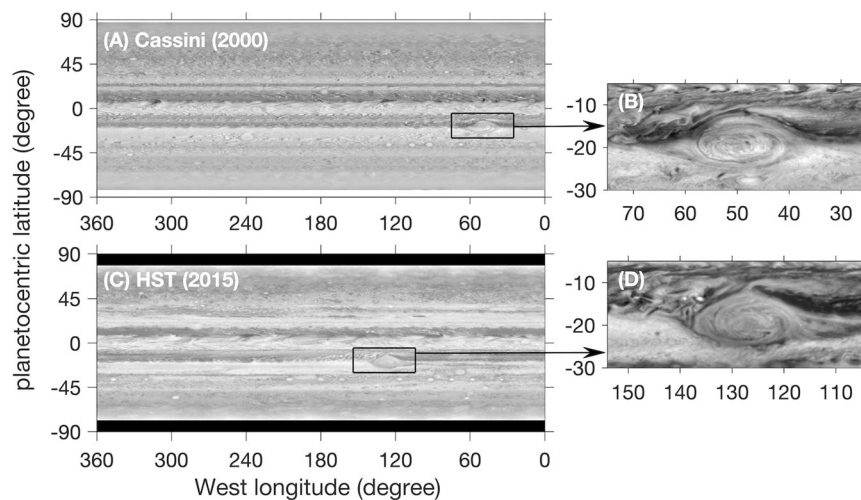


Fig. 9 Comparison of global maps between Cassini and HST. **(A)** A global map derived from images captured by Cassini ISS using the CB2 filter (750 nm) on December 13, 2000. The spatial resolution of these ISS/CB2 images ranges from ~ 100 km/pixel to ~ 120 km/pixel. **(B)** A global map derived from images captured by the HST WFC3 at a wavelength of 631 nm. These images were taken on January 9, 2015, with spatial resolutions varying between ~ 150 km/pixel and ~ 170 km/pixel.

We compared our global maps with previously published global maps. In a previous study¹⁹, the images recorded by the Hubble Space Telescope's Wide Field Camera 3 (HST WFC3) were used to make global maps. Figure 9 presents a comparison of global maps derived from Cassini ISS and HST WFC3 observations, highlighting a general consistency between the two. Differences in certain regional features can be attributed to variations in observational times, wavelengths, and spatial resolutions.

In particular, the Great Red Spot (GRS) is compared in both maps (see panels B and D in Fig. 9). First, the center of the GRS is located at $\sim 20^\circ$ S in both maps. This time-invariant latitudinal position is consistent with previous studies²⁰, which suggested that the GRS's latitude basically remains constant over time, despite temporal changes in other characteristics, such as shape, size, and drift velocity. More importantly, this consistency between Cassini and HST maps supports the accuracy of the navigation and mapping processes used for the global maps based on the images recorded by the Cassini ISS.

It is worth noting that the longitude of the GRS differs between the Cassini and HST maps due to its significant longitudinal drift driven by the background zonal winds²¹. Comparing Jupiter's global maps across different epochs not only helps validate these maps but also offers an opportunity to study the temporal evolution of dynamic atmospheric features like the GRS.

Finally, the project of creating global maps of Jupiter and Saturn based on the Cassini ISS images was supported by the NASA Data Archiving and Restoration Program. Before these datasets were publicly archived on the Planetary Atmospheres Node of the NASA PDS website, they underwent examination by experts at the Planetary Atmospheres Node and review by external referees. The PDS experts and external referees have thoroughly examined all aspects of the global maps, including the selection of ISS images, the map-making procedures, the format of the data products, and the associated documentation. Therefore, the datasets of global maps of Jupiter and Saturn are reliable.

Code availability

The Geological Survey Integrated Software for Imagers and Spectrometers (ISIS3), which was used to navigate the Cassini ISS images, is available at <https://isis.astrogeology.usgs.gov/7.0.0/UserStart/index.html>. The software Matlab was used for further processing of the Cassini ISS images, and guidelines for using Matlab can be found at <https://www.mathworks.com/products/matlab.html>. The Matlab codes for generating the global maps of Jupiter and Saturn are direct implementations of the methods introduced in this manuscript.

Received: 30 August 2024; Accepted: 2 January 2025;

Published online: 10 January 2025

References

- Jaffe, L. D. & Herrell, L. M. Cassini/Huygens science instruments, spacecraft, and mission. *Journal of spacecraft and rockets* **34**, 509–521, <https://doi.org/10.2514/2.3241> (1997).
- Porco, C. C., 19 colleagues. Cassini Imaging Science: Instrument characteristics and anticipated scientific investigations at Saturn. *Space Sci. Rev.* **115**, 363–497, <https://doi.org/10.1007/s11214-004-1456-7> (2004).
- Banfield, D. *et al.* Jupiter's cloud structure from Galileo imaging data. *Icarus* **135**, 230–250, <https://doi.org/10.1006/icar.1998.5985> (1998).
- Zhang, X., West, R. A., Banfield, D. & Yung, Y. L. Stratospheric aerosols on Jupiter from Cassini observations. *Icarus* **226**, 59–171, <https://doi.org/10.1016/j.icarus.2013.05.020> (2013).

5. Wong, M. H. *et al.* High-resolution UV/optical/IR imaging of Jupiter in 2016–2019. *The Astrophysical Journal Supplement Series* **247**, 58, <https://doi.org/10.3847/1538-4365/ab775f> (2020).
6. West, R. A. *et al.* Jupiter: The planet, satellites and magnetosphere. In: Bagenal, F., Dowling, T. E., McKinnon, W. B., Jewitt, D., Murray, C., Bell, J., Lorenz, R., Nimmo, F. (Eds.), Cambridge Planetary Science. Cambridge Univ. Press, New York, p. 81. 2004.
7. Minnaert, M. The reciprocity principle in lunar photometry. *The Astrophysical Journal* **93**, 403–410, <https://doi.org/10.1086/144279> (1941).
8. Vasavada, A. R. *et al.* Cassini imaging of Saturn: Southern hemisphere winds and vortices. *J. Geophys. Res.* **111**, <https://doi.org/10.1029/2005JE002563> (2006).
9. Trammell, H. J. *et al.* The global vortex analysis of Jupiter and Saturn based on Cassini Imaging Science Subsystem. *Icarus* **242**, 122–129, <https://doi.org/10.1016/j.icarus.2014.07.019> (2014).
10. Trammell, H. J. *et al.* Vortices in Saturn's Northern Hemisphere (2008–2015) observed by Cassini ISS. *Journal of Geophysical Research: Planets* **121**, 1814–1826, <https://doi.org/10.1002/2016JE005122> (2016).
11. Li, L., West, R., Jiang, X., and Knowles, B. Cassini ISS Global Maps of Jupiter and Saturn Bundle, NASA Planetary Data System, <https://doi.org/10.17189/rkkb-6y30> (2023).
12. Fischer, G. *et al.* A giant thunderstorm on Saturn. *Nature* **475**, 75–77, <https://doi.org/10.1038/nature10205> (2011).
13. Sanchez-Lavega, A. *et al.* Deep winds beneath Saturn's upper clouds from a seasonal long-lived planetary-scale storm. *Nature* **475**, 71–74, <https://doi.org/10.1038/nature10203> (2011).
14. Fletcher, L. N. *et al.* Thermal structure and dynamics of Saturn's northern springtime disturbance. *Science* **332**, 1413–1417, <https://doi.org/10.1126/science.1204774> (2011).
15. Sanchez-Lavega, A. *et al.* Ground-based observations of the long-term evolution and death of Saturn's Great White Spot. *Icarus* **220**, 561–576, <https://doi.org/10.1016/j.icarus.2012.05.033> (2012).
16. Sayanagi, K. M. *et al.* Dynamics of Saturn's great storm of 2010–2011 from Cassini ISS and RPWS. *Icarus* **223**, 460–478, <https://doi.org/10.1016/j.icarus.2012.12.013> (2013).
17. Garcia-Melendo, E. *et al.* Atmospheric dynamics of Saturn's 2010 giant storm. *Nature Geosciences* **23**, 525–529, <https://doi.org/10.1038/NGEO1860> (2013).
18. Li, L. *et al.* Unsymmetrical expansion of bright clouds from Saturn's 2010 Great White Storm, *Icarus*, <https://doi.org/10.1016/j.icarus.2021.114650> (2021).
19. Simon, A. A., Wong, M. H. & Orton, G. S. First results from the Hubble OPAL program: Jupiter in 2015. *The Astrophysical Journal* **812**, 55, <https://doi.org/10.1088/0004-637X/812/1/55> (2015).
20. Simon, A. A. *et al.* Historical and contemporary trends in the size, drift, and color of Jupiter's great red spot. *The Astronomical Journal* **155**, 151, <https://doi.org/10.3847/1538-3881/aaae01> (2018).
21. Simon, A. A., Wong, M. H., Marcus, P. S. & Irwin, P. G. A Detailed Study of Jupiter's Great Red Spot over a 90-day Oscillation Cycle. *The Planetary Science Journal* **5**, 223, <https://doi.org/10.3847/PSJ/ad71d1> (2024).

Acknowledgements

We are deeply grateful to the experts of the Planetary Atmospheres Node of the NASA Planetary Data System, Drs. Nancy Chanover, Lynn Neakrase, and Lyle Huber, for their invaluable assistance in archiving the datasets on the Planetary Data System and coordinating the external review. We also extend our gratitude to the three external reviewers invited by the NASA PDS for their constructive suggestions in improving the datasets. Additionally, we appreciate the Cassini ISS team for recording and organizing the raw datasets. Finally, we acknowledge the support received from the NASA ROSES Cassini Data Analysis Program, NSF Astronomy and Astrophysics Research Grants, and the Planetary Data Archiving, Restoration, and Tools Program.

Author contributions

L.L. and X.J. designed the research. X.W. conducted the data processing and map making. R.W. provided assistance in processing the Cassini ISS images.

Competing interests

The authors declare no competing interests.

Additional information

Correspondence and requests for materials should be addressed to X.W.

Reprints and permissions information is available at www.nature.com/reprints.

Publisher's note Springer Nature remains neutral with regard to jurisdictional claims in published maps and institutional affiliations.



Open Access This article is licensed under a Creative Commons Attribution-NonCommercial-NoDerivatives 4.0 International License, which permits any non-commercial use, sharing, distribution and reproduction in any medium or format, as long as you give appropriate credit to the original author(s) and the source, provide a link to the Creative Commons licence, and indicate if you modified the licensed material. You do not have permission under this licence to share adapted material derived from this article or parts of it. The images or other third party material in this article are included in the article's Creative Commons licence, unless indicated otherwise in a credit line to the material. If material is not included in the article's Creative Commons licence and your intended use is not permitted by statutory regulation or exceeds the permitted use, you will need to obtain permission directly from the copyright holder. To view a copy of this licence, visit <http://creativecommons.org/licenses/by-nc-nd/4.0/>.

© The Author(s) 2025